UCSF
UC San Francisco Previously Published Works

Title

Transformation of the Radial Glia Scaffold Demarcates Two Stages of Human Cerebral Cortex Development

Permalink

Journal

ISSN

Authors

Nowakowski, Tomasz J
Pollen, Alex A
Sandoval-Espinosa, Carmen
et al.

Publication Date

DOI

Peer reviewed

Transformation of the Radial Glia Scaffold Demarcates Two Stages of Human Cerebral Cortex Development

Tomasz J. Nowakowski[1,2,*], **Alex A. Pollen**[1,2], **Carmen Sandoval-Espinosa**[1,2], and **Arnold R. Kriegstein**[1,2,3,*]

[1]Eli and Edythe Broad Center of Regeneration Medicine and Stem Cell Research, University of California, San Francisco, San Francisco, CA 94143, USA

[2]Department of Neurology, University of California, San Francisco, San Francisco, CA 94158, USA

Abstract

The classic view of cortical development, embodied in the radial unit hypothesis highlights the ventricular radial glia (vRG) scaffold as a key architectonic feature of the developing neocortex. The scaffold includes continuous fibers spanning the thickness of the developing cortex during neurogenesis across mammals. However, we find that in humans, the scaffold transforms into a physically discontinuous structure during the transition from infragranular to supragranular neuron production. As a consequence of this transformation, supragranular layer neurons arrive at their terminal positions in the cortical plate along outer radial glia (oRG) cell fibers. In parallel, the radial glia that contact the ventricle develop a distinct "truncated" morphology and a unique gene expression profile. We propose a supragranular layer expansion hypothesis that posits a deterministic role of oRG cells in the radial and tangential expansion of supragranular layers in primates, with implications for patterns of neuronal migration, area patterning, and cortical folding.

Following sequential waves of induction and patterning of the neural tube, the cerebral cortical anlage emerges from the anterior neural tube. Around gestational week 7 (GW7) of human development, the founder population of neuroepithelial cells transforms into vRG cells that begin to divide asymmetrically to produce progeny that adopt neuronal fate directly, or reenter the cell cycle as intermediate progenitor cells (IPCs) (Bystron et al., 2006; Haubensak et al., 2004; Noctor et al., 2004). Upon differentiation, projection neurons migrate to their final destination in the cortical plate along the radial glia fiber scaffold (Rakic, 1972). The radial unit hypothesis postulates that neurons migrating along the same

or adjacent radial glia fibers form a cortical column, and that symmetric self-renewing divisions of vRG cells expand the founder population leading to additional cortical columns and tangential expansion of the cortical sheet (Rakic, 1978). This influential model provides a crucial framework for studying the development and evolution of the cerebral cortex. However, the radial unit hypothesis does not account for the increased complexity of radial glia progenitor populations in many species, the appearance of stereotyped cortical folds during neurogenesis, and the disproportionate expansion of upper cortical layers in the primate lineage.

Interestingly, previous studies observed that at late stages of human cortical development, around gestational week 18-19 (GW18-19) vRG cells no longer contact the pia and their processes terminate in the OSVZ (deAzevedo et al., 2003; Rakic and Sidman, 1968b; Sidman and Rakic, 1973). Similarly, radial glia cells that no longer contact the pial or ventricular surfaces have been reported in rhesus macaque starting from embryonic day 65, although periventricular astrocytes do not develop until E125, after the end of neurogenesis (Schmechel and Rakic, 1979). To provide further insights into the timing of the transformation of the radial glia scaffold in relation to the neurogenic time window, we visualized radial glia morphology during human cortical development using the lipophilic fluorescent dye DiI. At early stages of neurogenesis, prior to GW 16.5, placement of DiI on the ventricular surface revealed numerous cells with classical radial glia morphology, consisting of apical and basal processes spanning the entire thickness of the telencephalic wall (Figure 1A and S1). We term this the "continuous scaffold stage". In contrast, at later stages of neurogenesis (GW17-24), DiI labeling of the ventricular surface did not reveal cells with processes spanning the telencephalic wall (Figure 1A and S1-S2). Instead, radial glia displayed "truncated" morphologies (Rakic, 2003b), with fibers terminating abruptly in the OSVZ (Figure 1, S1 and S2). We term this the "discontinuous scaffold stage" and propose to refer to the radial glia population with non-classical morphologies as "truncated" radial glia ("tRG", Figure 1B). Because human cortical neurogenesis extends to the third trimester (Malik et al., 2013; Workman et al., 2013), the transformation of the radial glia scaffold into a physically discontinuous structure occurs midway through the neurogenic period.

To explore whether ventricular radial glia acquire a distinct molecular identity during their morphological transition to tRG cells, we reanalyzed patterns of gene expression in radial glia collected from primary human cortical samples (Camp et al., 2015; Pollen et al., 2015). Compared to radial glia at early stages (GW14-15) and oRG cells at later stages of cortical development (GW16-18), tRG cells retain the expression of pan-radial glia markers, such as PAX6, HES1, SLC1A3, and SOX2, but develop a distinct molecular profile characterized by reduced expression of genes such as FAM107A, LIFR, and HOPX, and enriched expression of genes such as CRYAB and NR4A1 (Figure 2A-C, S3A) (Pollen et al., 2015; Thomsen et al., 2016). Consistent with DiI labeling experiments, CRYAB-immunoreactive tRG fibers extend to the OSVZ but not beyond (Figure 2D, and Figure S2), and we identified many examples of tRG fibers oriented tangentially (Figure 2E arrows). The tRG fibers often terminate on capillaries, with their end-feet encircling endothelial cells, most prominently in the ISVZ and the inner portions of the OSVZ (Figure 2E arrowheads). Finally, we observed numerous SATB2 positive nuclei adjacent to tRG fibers (Figure 2F and S3B), suggesting a

role for tRGs in continuing to guide neuronal migration after the truncated fiber appears. Together, these observations indicate that at mid-neurogenesis, ventricular radial glia adopt a truncated morphology and a specific molecular program, supporting their distinction from classically-defined vRG cells.

Projection neurons that populate the distinct laminae of the cerebral cortex are produced sequentially, with deep layer neurogenesis preceding upper layer neurogenesis (Angevine and Sidman, 1961; Caviness and Rakic, 1978; Granger et al., 1995; Rakic, 1974). Studies in rodents, ferrets, and monkeys have shown that neuronal subtype specification may be determined at the level of radial glia cells, whose competence to produce diverse types of projection neurons becomes progressively restricted during development (Frantz and McConnell, 1996; Lukaszewicz et al., 2005; McConnell, 1988; McConnell and Kaznowski, 1991). In line with this prediction, genetic manipulations that extend radial glia neurogenesis in mouse result in an overproduction of upper cortical layer neurons (Nowakowski et al., 2013; Zhang et al., 2015). To relate the changes in radial glia scaffold organization to changes in the fate of neurons produced, we examined the identity of newborn neurons in the germinal zone using antibodies for the deep (infrangranular) cortical layer neuron markers, TBR1 and CTIP2, and for the marker SATB2, which is highly expressed in upper (supraganular) cortical layers. In the OSVZ of specimens younger than GW16.5, we observed prominent populations of neurons expressing TBR1, CTIP2, and SATB2 (Figure 3A). However, at stages corresponding to the discontinuous scaffold stage, we detected a prominent population of neurons expressing SATB2, but not TBR1 or CTIP2. Thus, the transformation of the radial glia scaffold from a continuous to a discontinuous structure closely parallels the well-established transition of radial glia from generating deep to generating upper layer neurons.

It has been proposed that an extended neurogenic time window underlies the radial expansion of supragranular layers in the primate lineage (Hutsler et al., 2005), and furthermore, that OSVZ progenitor cells contribute the majority of supragranular layer neurons in primates (Lukaszewicz et al., 2005; Smart et al., 2002). Indeed, the relative size of the OSVZ proliferative fraction increases as neurogenesis progresses in primates, while the frequency of mitoses in the ventricular zone decreases (Lukaszewicz et al., 2005; Martinez-Cerdeno et al., 2012; Rakic and Sidman, 1968a). Therefore, we examined whether changes in the radial glia scaffold correspond to the shift of radial glia proliferation to the OSVZ. Consistent with previous reports, we observed that the overall number of ventricular zone radial glia and mitotic figures declined towards mid-gestation, while the number of radial glia in the OSVZ steadily increased over the same period (Figure 3B-C). To examine whether the population of supragranular layer neurons continues to expand during the discontinuous scaffold stage, when oRG cells are the major proliferative population, we compared the proportion of supragranular and infragranular neurons at GW17-18 with GW23-24. The relative proportion of SATB2 positive neurons in the cortical plate at GW23-24 was significantly greater compared with GW17-18, even when migrating neurons in the intermediate zones were included in the GW17-18 cell number estimate (Figure 3D). Together, these findings suggest a shift in proliferative activity from ventricular to subventricular regions around the time of transition between the continuous and the discontinuous scaffold stages. Along with previous studies (Hansen et al., 2010; Pollen et

al., 2015), this also suggests that while oRG cells contribute to the production of both deep and upper cortical layer neurons, oRG cells may be especially important for the extended production of supragranular layer neurons in primates.

The expansion of the oRG population and the truncation of ventricular radial glia fibers at mid-neurogenesis suggest that oRG cells are sole contributors of the radial glia fibers guiding neurons to the cortical plate during supragranular layer neurogenesis. Indeed, DiI placement at the pial surface after GW16.5 labeled fibers terminating in cell bodies in the OSVZ, in contrast to experiments at earlier stages that also labeled cell bodies in the VZ (Figure 4 A). In addition, immunostaining experiments at GW18 demonstrated that the vast majority of VIM-expressing radial glia fibers in the intermediate zone (IZ) and the cortical plate (CP) co-expressed the recently described oRG marker, HOPX (Figure 4B). Recent studies suggest that oRG cells emerge as the daughter cells of horizontally dividing vRG cells and thereby inherit vRG basal fibers (LaMonica et al., 2013). This highlights a possible cellular mechanism by which the radial glia fibers that contact the pia in human cortex become progressively restricted to oRG cells. Future studies will be necessary to determine if all fibers of the founder vRG cells are inherited by oRG cells, and to establish if upon symmetric division of an oRG cell, both daughter oRG cells can establish basal fiber connections with the pial surface (Florio and Huttner, 2014). Consistent with previous findings (Hansen et al., 2010), we found rare examples of oRG cells with apical processes in our study (Figure S3C-D). Together, our observations suggest a revision of the radial unit hypothesis as it applies to primates, to include a transformation of the radial glia scaffold at mid-neurogenesis from a continuous structure to a discontinuous structure formed by two morphologically and molecularly distinct radial glia subtypes (Figure 4C).

The radial unit hypothesis advanced our understanding of the cytoarchitectonic organization of the developing neocortex. Symmetric divisions of the founder vRG cells increase the number of radial fibers reaching the pial surface, leading to a tangential expansion of the cortical plate (Chenn and Walsh, 2002; Haydar et al., 1999; Rakic, 1988). Subsequent models suggested that increases in OSVZ proliferation and oRG cell numbers could contribute to tangential expansion of the cortical plate leading to folding (Kriegstein et al., 2006; Reillo et al., 2011). The revised model presented here builds on these ideas to suggest that during supragranular layer neurogenesis in humans, the total number of oRG cell fibers directly predicts the surface area of the supragranular layers. One implication of this model is that during the discontinuous scaffold stage, neurogenic divisions of oRG cells expand supragranular layers radially, while self-renewing divisions of oRG cells expand supragranular layers tangentially. Because oRG expansion during the discontinuous scaffold stage occurs throughout human neocortical areas, the revised model provides a developmental mechanism for disproportional tangential expansion of supragranular cortex relative to infragranular cortex, which may broadly contribute to the folding of the cortical plate (Richman et al., 1975).

Recent studies also suggest that local expansion of OSVZ progenitors through increased generation or self-renewal may contribute to early stereotyped folding of the cortical plate (de Juan Romero et al., 2015; Dehay et al., 1996; Dehay et al., 1989; Dehay et al., 2001; Florio et al., 2015; Kriegstein et al., 2006; Nonaka-Kinoshita et al., 2013; Stahl et al., 2013;

Wang et al., 2016). In agreement with findings in the ferret cortex (Reillo and Borrell, 2012; Reillo et al., 2011), we observed fewer oRG cells underneath the human calcarine sulcus than the adjacent gyrus during mid-neurogenesis (Figure 4D). Interestingly, the ratio of IPCs to oRGs remained constant across gyri and sulci (Figure 4D), suggesting that the size of the oRG pool itself may regulate IPC abundance, as would be predicted from clonal lineage relationships (Hansen et al., 2010; Haubensak et al., 2004; Noctor et al., 2004). This early sculpting of stereotyped cortical folds through regulation of progenitor populations is compatible with later forces such as axonal tension and constrained cortical plate expansion guiding cortical folding (Mota and Herculano-Houzel, 2015; Sun and Hevner, 2014; Tallinen et al., 2016; Van Essen, 1997).

Radial glia play a fundamental role in orchestrating brain development, and congenital neurodevelopmental disorders such as microcephaly and lissencephaly have been linked to abnormalities in radial glia (Feng and Walsh, 2004; Gruber et al., 2011; Lancaster et al., 2013; Lizarraga et al., 2010; Pawlisz and Feng, 2011; Yingling et al., 2008). Transgenic mouse models of these disorders often show more subtle phenotypes than human patients, which may reflect important differences in radial glia development between these distantly related species. Future comparative studies of radial glia scaffold structure in a variety of species will be necessary to establish if the transformation of the radial glia scaffold at mid-neurogenesis is indeed primate-specific and related to cellular composition differences in upper layers, or if other mammals with large cortices share this shift in cytoarchitecture. The radial glia scaffold in the developing ferret cortex remains continuous throughout neurogenesis despite pronounced folding and expanded upper layers relative to mouse (Borrell, 2010; Reillo et al., 2011), but other mammals with folded cortices have not been examined. Therefore the full biological significance of the radial glia scaffold transformation remains to be explored.

The updated model of human cortical development outlined here has several implications for understanding patterns of neuronal migration and regionalization of the cortex, as well as connectivity of supragranular layer neurons during human cerebral cortex development. The model predicts that supragranular layer neurons born during the discontinuous scaffold stage migrate towards the cortical plate almost exclusively along oRG fibers. Because interactions between radial glia fibers and migrating neurons can impact cortical development (Elias et al., 2007; Ohtaka-Maruyama and Okado, 2015), future studies will be needed to explore whether the signals mediated by oRG basal fibers are different than those mediated by vRG and tRG fibers. In addition, increased dispersion of neurons during the discontinuous scaffold stage in primate cortex suggests that the ontogenetic relationship between supragranular layer neurons in the same cortical column would be more diverse than between infragranular layer neurons, which might have implications for establishing cortical connectivity (Yu et al., 2009). Finally, the protomap hypothesis postulates that cortical area information may be initially encoded by genetic factors in the ventricular zone (Rakic, 1988), although the map may be refined by thalamocortical innervation and sensory input (O'Leary, 1989; Rakic, 1988). The expansion of supragranular layers at stages when tRG cells are no longer a significant source of newborn neurons or of basal processes reaching the cortical plate suggests that oRG cells may retain positional information related to cortical area identity. Recent work suggests that astrocyte populations in the cerebral cortex may also

be regionally restricted (Tsai et al., 2012), implying that positional information may be further retained in glia after the dissolution of the radial glia scaffold.

Our current understanding of the dynamic features of the radial glia scaffold supports a revised model of primate cerebral cortex development (Figure 5). During infragranular layer neurogenesis, when many of the neuronal types highly conserved in mammals, such as corticothalamic, corticospinal, and corticobulbar projection neurons are generated, both vRG and oRG cells are present in the germinal zone and can support radial migration. After approximately GW17 of human development, vRG cells lose pia contacting basal processes and transform into tRG cells, and newborn supragranular neurons, that establish intracortical associative and commissural projections, migrate to the cortical plate along oRG cell fibers. This updated model thus suggests a cellular mechanism for developmental and evolutionary expansion of the supragranular layers that are thought to be responsible for many of the cognitive features unique to primates.

Experimental Procedures

De-identified tissue samples were collected with previous patient consent in strict observance of the legal and institutional ethical regulations. Protocols were approved by the Human Gamete, Embryo and Stem Cell Research Committee (institutional review board) at the University of California, San Francisco. Primary tissue samples were dissected in artificial cerebrospinal fluid containing 125 mM NaCl, 2.5 mM KCl, 1 mM $MgCl_2$, 1 mM $CaCl_2$, 1.25 mM NaH_2PO_4 and fixed overnight in 4% paraformaldehyde prepared in phosphate buffered saline.

For labeling with DiI (Thermo Fisher), fixed chunks of cortical tissue samples were transferred to a dish and DiI crystals were placed against the pial, ventricular, or OSVZ surfaces, as indicated in figure legends or figure panels. The samples were then incubated in 4% paraformaldehyde for 7 days (specimens younger than GW20) or 10 days (GW24 specimen) at 37°C. GW19 sample used to visualize dye diffusion along axonal fiber tracts was incubated for 6 days at 37°C. For all analyzed samples, we inspected the tissue block under fluorescent illumination initially to assess the continuity of the radial glia scaffold. Tissue samples were then serially sectioned perpendicular to the ventricle to 500 μm slices using a Leica VT1200S vibrating blade microtome in ice cold PBS. All consecutive sections were analyzed under epifluorescent microscope to assess continuity of the radial glia scaffold through the thickness of the tissue. Representative images of the longest observed fibers were collected using Leica TCS SP5 X Confocal microscope and processed in Photoshop (Adobe) to obtain black and white inverted images for better visualization of the positive staining. Analysis was performed on a total of 11 primary tissue samples, aged GW14 (n=1), GW15 (n=1), GW15.5 (n=2), GW16.5 (n=1), GW17 (n=2), GW18 (n=2), GW19 (n=1), GW19.5 (n=1), and GW24 (n=1). Multiple consecutive 500 μm slices through GW16.5, GW17, and GW24 are shown in Figures S1 and S2 to ascertain that the reported absence of pia contacting vRG cells after GW16.5 is not a sectioning artifact.

For immunohistochemical detection of protein expression, tissue samples were cryoprotected in 30% sucrose/PBS and frozen in a 1:1 mixture of 30% sucrose and optimum

cutting temperature compound (Tissue-Tek). Thin 20μm sections were collected using Leica CM3050 S cryostat. Antigen retrieval was performed in 10 mM sodium citrate buffer at pH=6. Primary antibodies against CD31 (1:100, Abcam ab76533), CRYAB (1:100, Abcam ab13496), CTIP2 (1:500, Abcam ab18465), phosphorylated histone H3 (1:100, Cell Signaling #9706), HOPX (1:100, Santa Cruz Biotechnology sc-30216), NR4A1 (1:100, Aviva Systems Biology ARP45604_P050), SATB2 (1:250, Santa Cruz Biotechnology sc-81376), SOX2 (1:200, Santa Cruz Biotechnology sc-17320), TBR1 (1:100, Abcam ab31940), VIM (1:100, Millipore AB5733) were used in this study. Blocking and antibody incubations were performed in the presence of 0.2% gelatin, 10% donkey serum, and 1% Triton X-100. Primary antibody was detected using a suitable fluorophore-conjugated donkey secondary antibody AlexaFluor (Life Technologies). Cell nuclei were counter-stained using DAPI (Life Technologies) and sections were mounted in Aqua-mount (Lerner Laboratories). Images were collected using a Leica TCS SP5 X Confocal microscope.

Quantification of cells immunopositive for phospho-Histone H3 and SOX2, as well as HOPX and EOMES shown in Figure 2 was performed manually in Photoshop in two non-adjacent regions from independent sections for each of the specimens. Counting was performed without previous knowledge of the sample age. A rectangular counting box (500 μm wide) was placed perpendicular to the ventricular edge. Anatomical region (VZ, ISVZ, and OSVZ) was determined based on nuclear density. Quantification of HOPX and VIM co-expression shown in Figure 1 was performed in Photoshop (Adobe). Narrow counting boxes (500 μm by 50 μm) were positioned over an image of VIM staining so that the 500 μm is approximately perpendicular to the radial glia fibers. For each image, one box was placed in the IZ and one in the CP. Varicosities of the radial glia fibers were marked based on VIM immunohistochemistry and then examined for HOPX staining. For each of the four biological replicates, two non-adjacent sections were chosen at random.

Quantification of projection neuron markers TBR1, CTIP2 and SATB2 shown in Figure 3 was performed in Imaris (Bitplane). For each biological replicate, two nonadjacent sections were analyzed by placing a 500 μm counting area spanning the thickness of the cortical plate. For samples aged GW17-18, we included subplate and the IZ in the counting region to include radially migrating neurons in the estimate of the size neuronal populations present at that age.

Single cell mRNA sequencing data (Camp et al., 2015; Pollen et al., 2015) were downloaded from data repositories and processed as described before (Pollen et al., 2015). Previously annotated vRG and oRG classifications were used for GW16-18 "late" radial glia types (Pollen et al., 2015). To identify GW14-15 "early" radial glia (Camp et al., 2015), hierarchical clustering of samples across key genes used for cell type classification in the developing human cortex (Pollen et al., 2015) was performed to identify cells with correlated expression of canonical radial glia markers and the absence of neuronal, intermediate progenitor, and interneuron enriched genes. Principal Component Analysis was used to identify 1000 genes most strongly contributing to transcriptional variation across principal components 1-5. Weighted Gene Coexpression Network Analysis was performed following published manual using default settings (Langfelder and Horvath, 2008). Gene modules were identified using 'dynamicTreeCut' package at deepSplit=2. To identify gene

modules correlated with vRG and oRG cells, Pearson's correlation value was calculated between module eigengene and an "ideal" vector with value of 1 across the cell of a given type.

Supplementary Material

Refer to Web version on PubMed Central for supplementary material.

Acknowledgement

References

Angevine JB Jr. Sidman RL. Autoradiographic study of cell migration during histogenesis of cerebral cortex in the mouse. Nature. 1961; 192:766–768.

Betizeau M, Cortay V, Patti D, Pfister S, Gautier E, Bellemin-Menard A, Afanassieff M, Huissoud C, Douglas RJ, Kennedy H, et al. Precursor diversity and complexity of lineage relationships in the outer subventricular zone of the primate. Neuron. 2013; 80:442–457. [PubMed: 24139044]

Borrell V. In vivo gene delivery to the postnatal ferret cerebral cortex by DNA electroporation. Journal of neuroscience methods. 2010; 186:186–195. [PubMed: 19944720]

Bystron I, Rakic P, Molnar Z, Blakemore C. The first neurons of the human cerebral cortex. Nature neuroscience. 2006; 9:880–886. [PubMed: 16783367]

Camp JG, Badsha F, Florio M, Kanton S, Gerber T, Wilsch-Brauninger M, Lewitus E, Sykes A, Hevers W, Lancaster M, et al. Human cerebral organoids recapitulate gene expression programs of fetal neocortex development. Proceedings of the National Academy of Sciences of the United States of America. 2015; 112:15672–15677. [PubMed: 26644564]

Caviness VS Jr. Rakic P. Mechanisms of cortical development: a view from mutations in mice. Annual review of neuroscience. 1978; 1:297–326.

Chenn A, Walsh CA. Regulation of cerebral cortical size by control of cell cycle exit in neural precursors. Science. 2002; 297:365–369. [PubMed: 12130776]

de Juan Romero C, Bruder C, Tomasello U, Sanz-Anquela JM, Borrell V. Discrete domains of gene expression in germinal layers distinguish the development of gyrencephaly. The EMBO journal. 2015; 34:1859–1874. [PubMed: 25916825]

deAzevedo LC, Fallet C, Moura-Neto V, Daumas-Duport C, Hedin-Pereira C, Lent R. Cortical radial glial cells in human fetuses: depth-correlated transformation into astrocytes. Journal of neurobiology. 2003; 55:288–298. [PubMed: 12717699]

Dehay C, Giroud P, Berland M, Killackey H, Kennedy H. Contribution of thalamic input to the specification of cytoarchitectonic cortical fields in the primate: effects of bilateral enucleation in the fetal monkey on the boundaries, dimensions, and gyrification of striate and extrastriate cortex. The Journal of comparative neurology. 1996; 367:70–89. [PubMed: 8867284]

Dehay C, Horsburgh G, Berland M, Killackey H, Kennedy H. Maturation and connectivity of the visual cortex in monkey is altered by prenatal removal of retinal input. Nature. 1989; 337:265–267. [PubMed: 2536139]

Dehay C, Savatier P, Cortay V, Kennedy H. Cell-cycle kinetics of neocortical precursors are influenced by embryonic thalamic axons. The Journal of neuroscience : the official journal of the Society for Neuroscience. 2001; 21:201–214. [PubMed: 11150337]

Elias LA, Wang DD, Kriegstein AR. Gap junction adhesion is necessary for radial migration in the neocortex. Nature. 2007; 448:901–907. [PubMed: 17713529]

Feng Y, Walsh CA. Mitotic spindle regulation by Nde1 controls cerebral cortical size. Neuron. 2004; 44:279–293. [PubMed: 15473967]

Florio M, Albert M, Taverna E, Namba T, Brandl H, Lewitus E, Haffner C, Sykes A, Wong FK, Peters J, et al. Human-specific gene ARHGAP11B promotes basal progenitor amplification and neocortex expansion. Science. 2015; 347:1465–1470. [PubMed: 25721503]

Florio M, Huttner WB. Neural progenitors, neurogenesis and the evolution of the neocortex. Development. 2014; 141:2182–2194. [PubMed: 24866113]

Frantz GD, McConnell SK. Restriction of late cerebral cortical progenitors to an upper-layer fate. Neuron. 1996; 17:55–61. [PubMed: 8755478]

Granger B, Tekaia F, Le Sourd AM, Rakic P, Bourgeois JP. Tempo of neurogenesis and synaptogenesis in the primate cingulate mesocortex: comparison with the neocortex. The Journal of comparative neurology. 1995; 360:363–376. [PubMed: 8522653]

Gruber R, Zhou Z, Sukchev M, Joerss T, Frappart PO, Wang ZQ. MCPH1 regulates the neuroprogenitor division mode by coupling the centrosomal cycle with mitotic entry through the Chk1-Cdc25 pathway. Nature cell biology. 2011; 13:1325–1334. [PubMed: 21947081]

Hansen DV, Lui JH, Parker PR, Kriegstein AR. Neurogenic radial glia in the outer subventricular zone of human neocortex. Nature. 2010; 464:554–561. [PubMed: 20154730]

Haubensak W, Attardo A, Denk W, Huttner WB. Neurons arise in the basal neuroepithelium of the early mammalian telencephalon: a major site of neurogenesis. Proceedings of the National Academy of Sciences of the United States of America. 2004; 101:3196–3201. [PubMed: 14963232]

Haydar TF, Kuan CY, Flavell RA, Rakic P. The role of cell death in regulating the size and shape of the mammalian forebrain. Cerebral cortex. 1999; 9:621–626. [PubMed: 10498280]

Hutsler JJ, Lee DG, Porter KK. Comparative analysis of cortical layering and supragranular layer enlargement in rodent carnivore and primate species. Brain research. 2005; 1052:71–81. [PubMed: 16018988]

Kriegstein A, Noctor S, Martinez-Cerdeno V. Patterns of neural stem and progenitor cell division may underlie evolutionary cortical expansion. Nature reviews Neuroscience. 2006; 7:883–890. [PubMed: 17033683]

Lancaster MA, Renner M, Martin CA, Wenzel D, Bicknell LS, Hurles ME, Homfray T, Penninger JM, Jackson AP, Knoblich JA. Cerebral organoids model human brain development and microcephaly. Nature. 2013; 501:373–379. [PubMed: 23995685]

Langfelder P, Horvath S. WGCNA: an R package for weighted correlation network analysis. BMC bioinformatics. 2008; 9:559. [PubMed: 19114008]

Lizarraga SB, Margossian SP, Harris MH, Campagna DR, Han AP, Blevins S, Mudbhary R, Barker JE, Walsh CA, Fleming MD. Cdk5rap2 regulates centrosome function and chromosome segregation in neuronal progenitors. Development. 2010; 137:1907–1917. [PubMed: 20460369]

Lukaszewicz A, Savatier P, Cortay V, Giroud P, Huissoud C, Berland M, Kennedy H, Dehay C. G1 phase regulation, area-specific cell cycle control, and cytoarchitectonics in the primate cortex. Neuron. 2005; 47:353–364. [PubMed: 16055060]

Malik S, Vinukonda G, Vose LR, Diamond D, Bhimavarapu BB, Hu F, Zia MT, Hevner R, Zecevic N, Ballabh P. Neurogenesis continues in the third trimester of pregnancy and is suppressed by premature birth. The Journal of neuroscience : the official journal of the Society for Neuroscience. 2013; 33:411–423. [PubMed: 23303921]

Martinez-Cerdeno V, Cunningham CL, Camacho J, Antczak JL, Prakash AN, Cziep ME, Walker AI, Noctor SC. Comparative analysis of the subventricular zone in rat, ferret and macaque: evidence for an outer subventricular zone in rodents. PloS one. 2012; 7:e30178. [PubMed: 22272298]

McConnell SK. Fates of visual cortical neurons in the ferret after isochronic and heterochronic transplantation. The Journal of neuroscience : the official journal of the Society for Neuroscience. 1988; 8:945–974. [PubMed: 3346731]

McConnell SK, Kaznowski CE. Cell cycle dependence of laminar determination in developing neocortex. Science. 1991; 254:282–285. [PubMed: 1925583]

Mota B, Herculano-Houzel S. BRAIN STRUCTURE. Cortical folding scales universally with surface area and thickness, not number of neurons. Science. 2015; 349:74–77. [PubMed: 26138976]

Noctor SC, Martinez-Cerdeno V, Ivic L, Kriegstein AR. Cortical neurons arise in symmetric and asymmetric division zones and migrate through specific phases. Nature neuroscience. 2004; 7:136–144. [PubMed: 14703572]

Nonaka-Kinoshita M, Reillo I, Artegiani B, Martinez-Martinez MA, Nelson M, Borrell V, Calegari F. Regulation of cerebral cortex size and folding by expansion of basal progenitors. The EMBO journal. 2013; 32:1817–1828. [PubMed: 23624932]

Nowakowski TJ, Mysiak KS, O'Leary T, Fotaki V, Pratt T, Price DJ. Loss of functional Dicer in mouse radial glia cell-autonomously prolongs cortical neurogenesis. Developmental biology. 2013

O'Leary DD. Do cortical areas emerge from a protocortex? Trends in neurosciences. 1989; 12:400–406. [PubMed: 2479138]

Ohtaka-Maruyama C, Okado H. Molecular Pathways Underlying Projection Neuron Production and Migration during Cerebral Cortical Development. Frontiers in neuroscience. 2015; 9:447. [PubMed: 26733777]

Pawlisz AS, Feng Y. Three-dimensional regulation of radial glial functions by Lis1-Nde1 and dystrophin glycoprotein complexes. PLoS biology. 2011; 9:e1001172. [PubMed: 22028625]

Pollen AA, Nowakowski TJ, Chen J, Retallack H, Sandoval-Espinosa C, Nicholas CR, Shuga J, Liu SJ, Oldham MC, Diaz A, et al. Molecular Identity of Human Outer Radial Glia during Cortical Development. Cell. 2015; 163:55–67. [PubMed: 26406371]

Rakic P. Mode of cell migration to the superficial layers of fetal monkey neocortex. The Journal of comparative neurology. 1972; 145:61–83. [PubMed: 4624784]

Rakic P. Neurons in rhesus monkey visual cortex: systematic relation between time of origin and eventual disposition. Science. 1974; 183:425–427. [PubMed: 4203022]

Rakic P. Neuronal migration and contact guidance in the primate telencephalon. Postgraduate medical journal. 1978; 54(Suppl 1):25–40.

Rakic P. Specification of cerebral cortical areas. Science. 1988; 241:170–176. [PubMed: 3291116]

Rakic P. Developmental and evolutionary adaptations of cortical radial glia. Cerebral cortex. 2003a; 13:541–549.

Rakic P. Elusive radial glial cells: historical and evolutionary perspective. Glia. 2003b; 43:19–32. [PubMed: 12761862]

Rakic P, Sidman RL. Autoradiographic study of supravital DNA synthesis in fetal human brain. Journal of neuropathology and experimental neurology. 1968a; 27:139–140.

Rakic P, Sidman RL. Supravital DNA synthesis in the developing human and mouse brain. Journal of neuropathology and experimental neurology. 1968b; 27:246–276. [PubMed: 5646196]

Reillo I, Borrell V. Germinal zones in the developing cerebral cortex of ferret: ontogeny, cell cycle kinetics, and diversity of progenitors. Cerebral cortex. 2012; 22:2039–2054. [PubMed: 21988826]

Reillo I, de Juan Romero C, Garcia-Cabezas MA, Borrell V. A role for intermediate radial glia in the tangential expansion of the mammalian cerebral cortex. Cerebral cortex. 2011; 21:1674–1694. [PubMed: 21127018]

Richman DP, Stewart RM, Hutchinson JW, Caviness VS Jr. Mechanical model of brain convolutional development. Science. 1975; 189:18–21. [PubMed: 1135626]

Schmechel DE, Rakic P. Arrested proliferation of radial glial cells during midgestation in rhesus monkey. Nature. 1979; 277:303–305. [PubMed: 105294]

Sidman RL, Rakic P. Neuronal migration, with special reference to developing human brain: a review. Brain research. 1973; 62:1–35. [PubMed: 4203033]

Smart IH, Dehay C, Giroud P, Berland M, Kennedy H. Unique morphological features of the proliferative zones and postmitotic compartments of the neural epithelium giving rise to striate and extrastriate cortex in the monkey. Cerebral cortex. 2002; 12:37–53. [PubMed: 11734531]

Stahl R, Walcher T, De Juan Romero C, Pilz GA, Cappello S, Irmler M, Sanz-Aquela JM, Beckers J, Blum R, Borrell V, et al. Trnp1 regulates expansion and folding of the mammalian cerebral cortex by control of radial glial fate. Cell. 2013; 153:535–549. [PubMed: 23622239]

Sun T, Hevner RF. Growth and folding of the mammalian cerebral cortex: from molecules to malformations. Nature reviews Neuroscience. 2014; 15:217–232. [PubMed: 24646670]

Takahashi T, Nowakowski RS, Caviness VS Jr. Cell cycle parameters and patterns of nuclear movement in the neocortical proliferative zone of the fetal mouse. The Journal of neuroscience : the official journal of the Society for Neuroscience. 1993; 13:820–833. [PubMed: 8426239]

Tallinen T, Chung JY, Rousseau F, Girard N, Lefevre J, Mahadevan L. On the growth and form of cortical convolutions. Nat Phys. 2016 advance online publication.

Thomsen ER, Mich JK, Yao Z, Hodge RD, Doyle AM, Jang S, Shehata SI, Nelson AM, Shapovalova NV, Levi BP, et al. Fixed single-cell transcriptomic characterization of human radial glial diversity. Nature methods. 2016; 13:87–93. [PubMed: 26524239]

Tsai HH, Li H, Fuentealba LC, Molofsky AV, Taveira-Marques R, Zhuang H, Tenney A, Murnen AT, Fancy SP, Merkle F, et al. Regional astrocyte allocation regulates CNS synaptogenesis and repair. Science. 2012; 337:358–362. [PubMed: 22745251]

Van Essen DC. A tension-based theory of morphogenesis and compact wiring in the central nervous system. Nature. 1997; 385:313–318. [PubMed: 9002514]

Wang L, Hou S, Han Y-G. Hedgehog signaling promotes basal progenitor expansion and the growth and folding of the neocortex. Nature neuroscience. 2016 advance online publication.

Workman AD, Charvet CJ, Clancy B, Darlington RB, Finlay BL. Modeling transformations of neurodevelopmental sequences across mammalian species. The Journal of neuroscience : the official journal of the Society for Neuroscience. 2013; 33:7368–7383. [PubMed: 23616543]

Yingling J, Youn YH, Darling D, Toyo-Oka K, Pramparo T, Hirotsune S, Wynshaw-Boris A. Neuroepithelial stem cell proliferation requires LIS1 for precise spindle orientation and symmetric division. Cell. 2008; 132:474–486. [PubMed: 18267077]

Yu YC, Bultje RS, Wang X, Shi SH. Specific synapses develop preferentially among sister excitatory neurons in the neocortex. Nature. 2009; 458:501–504. [PubMed: 19204731]

Zhang C, Ge X, Liu Q, Jiang M, Li MW, Li H. MicroRNA-mediated non-cell-autonomous regulation of cortical radial glial transformation revealed by a Dicer1 knockout mouse model. Glia. 2015; 63:860–876. [PubMed: 25643827]

Radial glia fibers form a physical scaffold that supports neuronal migration during neurogenesis. During human neurogenesis, this scaffold transforms into a physically discontinuous structure formed by two morphologically and molecularly distinct radial glia subtypes: truncated and outer radial glia.

- Radial glia scaffold of the human brain becomes discontinuous at mid-neurogenesis

- Ventricle-contacting truncated radial glia develop distinct molecular identity

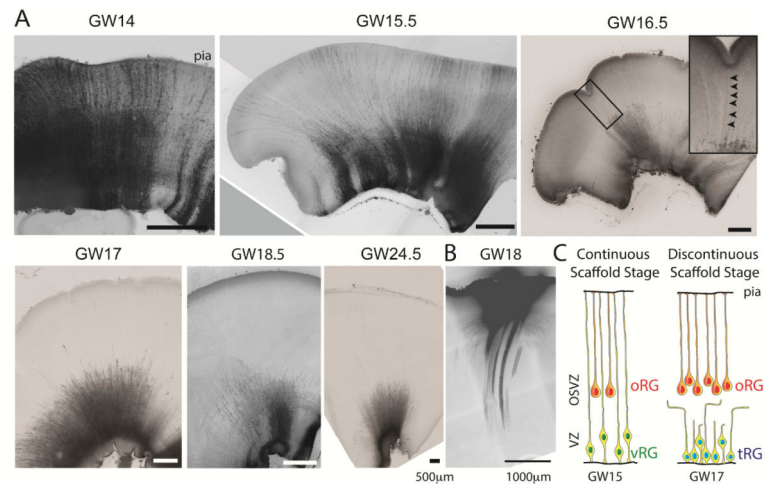- The radial glia scaffold is discontinuous during supragranular layer neurogenesis

Figure 1. Morphological Transition in Radial Glia Scaffold During Human Cortical Development

(A) DiI labeling of cells contacting the ventricular surface throughout neurogenesis reveals continuous radial glia scaffold prior to GW16.5, but only shorter "truncated" processes after GW16.5. Arrows indicate sporadic examples of individual fibers extending to the pial surface at GW16.5. See also Figure S1 and S2 for additional examples. **(B)** Conversely, DiI placement at the pial surface at GW18 labeled fibers extending to the OSVZ, but no ventricular surface contacting cells (See also Figures 3, S4). **(C)** Schematic representing three major classes of radial glia cells: classical ventricular radial glia (vRG) with fibers extending to the pial surface, ventricle contacting "truncated" radial glia (tRG) with non-classical morphologies whose processes terminate in the OSVZ, and outer radial glia (oRG).
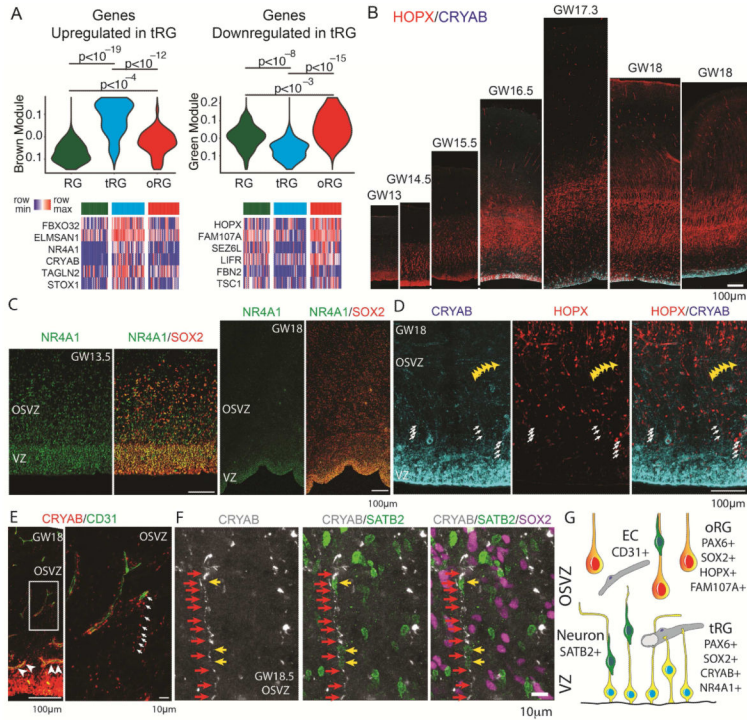
Figure 2. Molecular Identity of Truncated Radial Glia

(A) Violin plots represent distribution of module eigengene values for gene correlation networks upregulated in tRG (module "brown") and specifically downregulated in tRG cells (module "green"), across previously published single cell RNA-Seq datasets generated for 39 GW14-15 radial glia (RG), 48 GW16-18 tRG cells (previously referred to as vRG cells), and 46 GW16-18 oRG cells (Camp et al., 2015; Pollen et al., 2015). Heatmaps show normalized expression values of representative members of both modules across single cells (see also Supplementary Table 1 for gene module assignments and information about the number of cells of in each class). p-values were calculated using two-way Student t-test. **(B)** Staining of primary tissue sections for the oRG marker, HOPX and a tRG marker, CRYAB, showing rapid onset of CRYAB expression at around GW16.5. **(C)** NR4A1 expression is enriched in the VZ during early stages of cortical development and in tRG cells. **(D)** Representative high magnification image of CRYAB and HOPX immunostaining in the germinal zone. Arrows indicate CRYAB positive tRG fibers and yellow arrowheads indicate an example of a tangentially oriented CRYAB positive fiber consistent with the late tRG fiber morphologies shown in Figure 1. **(E)** Immunostaining of human germinal zone revealing association of tRG fibers with blood capillaries. Arrowheads indicate examples of CD31-positive endothelial cells surrounded by CRYAB immunostaining of tRG cells. Arrows in the magnified image from the OSVZ highlight an example of a tRG fiber reaching a blood capillary. **(F)** Representative example of a CRYAB positive tRG fiber in a GW18.5 sample. Red arrows highlight a CRYAB positive fiber and yellow arrows indicate SATB2 positive neuronal cell bodies juxtaposed to the tRG fiber. See also Figure S3 for an example from a GW18.2 specimen. **(G)** Proposed features of tRG cells include truncated morphology

of the basal fiber, distinct molecular identity, and frequent association with blood vessels (EC – endothelial cell).
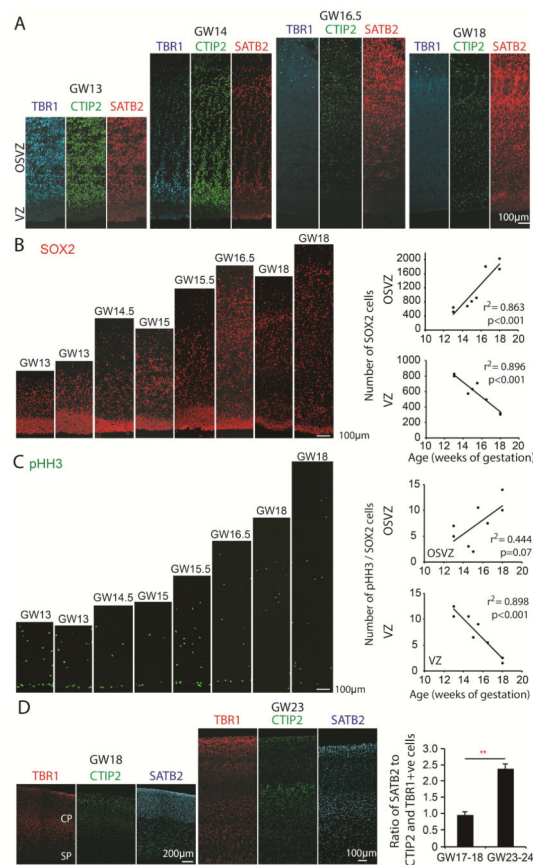
Figure 3. Expansion of Supragranular Layers During the Discontinuous Stage of Cortical Development

(A) Immunohistochemical detection of newborn neurons in the cortical germinal zone using antibodies for cortical layer markers. **(B,C)** Immunolabeling and quantification of the total number of SOX2+ cells. **(B)** SOX2+ cells and phosphorylated Histone H3 and SOX2 double-positive cells (**C**), in the VZ and OSVZ between GW13 and GW18. The non-linear increase in oRG cell mitoses may reflect dynamic changes in cell cycle parameters over the course of cortical development (Betizeau et al., 2013; Takahashi et al., 1993). Scatter plots represent quantification results of average total number of immunopositive cells for each primary tissue sample shown in the overlying images. Each data point represents a distinct biological replicate, and the quantification was performed in two randomly selected non-adjacent tissue sections, as outlined in Experimental Procedures. Statistical significance was evaluated using linear regression test with p-values displayed above the graph. **(D)** Left and middle panels show representative examples of immunohistochemical detection of cortical projection neurons around GW18 (left) and GW24 (middle) using antibodies against markers of laminar identity TBR1, CTIP2 (expressed in deep layer neurons), and SATB2 (expressed in upper layer neurons). Quantification of neuronal populations at GW17-18 (n=3, quantification included cortical plate CP and regions containing migrating neurons, IZ and subplate, SP) and at GW 23-24 (n=3). ** - p<0.01, Student's t-test. Error bars represent s.e.m.
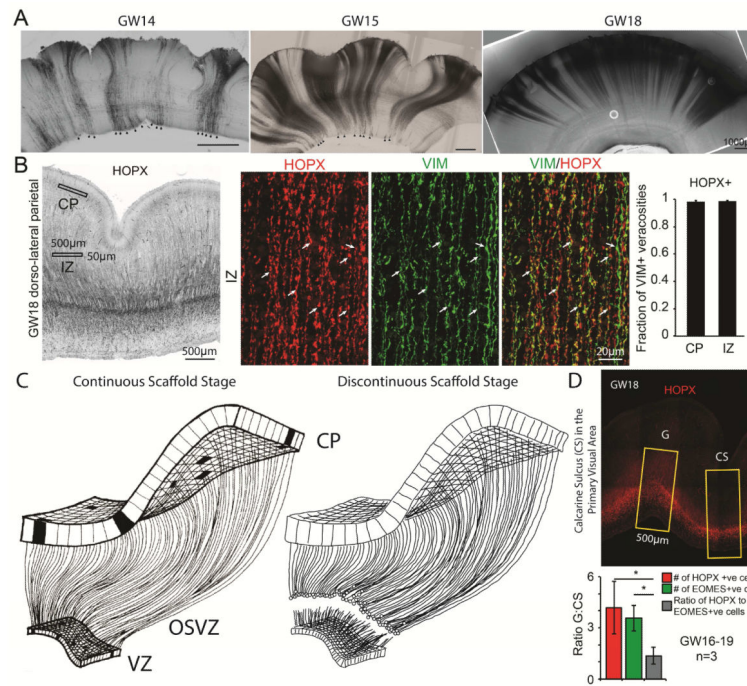
Figure 4. Radial Glia Scaffold Reaching the Cortical Plate During Supragranular Layer Neurogenesis is Formed by oRG Cells

(A) DiI labeling of pia contacting cells throughout human neurogenesis. Consistent with the proposed model, no back-labeled of ventricle contacting cells (arrowheads in left and middle panel) are observed after GW16.5. Note that any apparent folding of the tissue may represent tissue processing artifacts. **(B)** Validation of cell identity of radial glia fibers in the intermediate zone (IZ) and the cortical plate (CP) using immunohistochemistry. Left image shows representative immunostaining for HOPX, while panels show high magnification example of a fraction of a counting area in the IZ. Arrows indicate varicosities double positive for the pan radial glia marker, VIM, and the outer radial glia marker, HOPX. Quantification represents n=4 (GW17-18.5) biological replicates, error bars represent s.e.m. **(C)** Two stages of human cerebral cortex development during neurogenesis. Left panel with permission from (Rakic, 2003a). **(D)** Representative example of HOPX immunostaining of a tissue section through the calcarine sulcus ("CS") and the adjacent gyrus ("G") for the oRG marker, HOPX. Quantification was performed in three biological replicates (GW16, GW18, and GW19), total numbers of HOPX and EOMES immunopositive cells in the OSVZ was quantified across two randomly selected non-adjacent tissue sections, as outlined in Experimental Procedures. Bar graph represents the average ratios of OSVZ oRG cells (red bar), IPCs (green bar), and a relative abundance of oRGs to IPCs (gray bar) between the gyrus and the calcarine sulcus. * - p<0.05, paired Student's t-test. Error bars represent s.e.m.
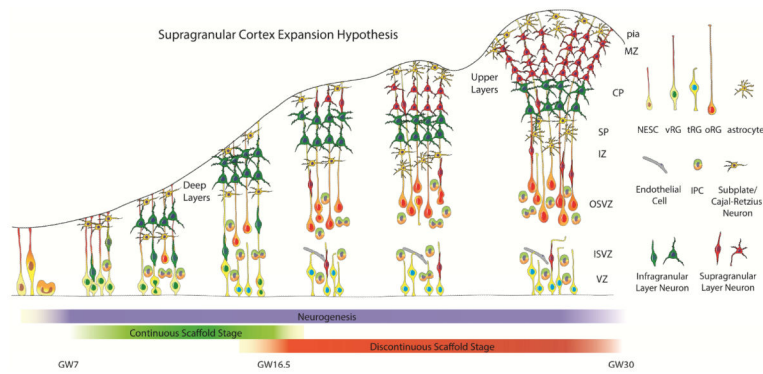
Figure 5. The Supragranular Cortex Expansion Hypothesis
By integrating experimental evidence in the published literature with our experimental
findings we propose that primate cortical neurogenesis can be divided into two stages.
During early neurogenesis (left), basal fibers of ventricular radial glia contact the pial
surface and newborn neurons migrate along ventricular as well as outer radial glia fibers.
During late neurogenesis (right), newborn neurons reach the cortical plate only along outer
radial glia fibers. VZ – ventricular zone, NESC – neuroepithelial stem cell, ISVZ – inner
subventricular zone, OSVZ – outer subventricular zone, IZ – intermediate zone, SP –
subplate, CP – cortical plate, MZ – marginal zone, IPC – intermediate progenitor cell, vRG
– ventricular radial glia, tRG – truncated radial glia, oRG – outer radial glia.